Blended Hybrids Based on Silsesquioxane–OH and Epoxy Resins

Tingli Lu,[1] Guozheng Liang,[2] Yaoli Peng,[3] Tao Chen[1]

[1]*Faculty of Life Science, Northwestern Polytechnical University, Xi'an, Shaanxi 710072, People's Republic of China*
[2]*School of Material Engineering, Soochow University, Suzhou, Jiangsu 215006, People's Republic of China*
[3]*School of Chemical Engineering and Technology, China University of Mining and Technology, Xuzhou, Jiangsu 221008, People's Republic of China*

ABSTRACT: Blended hybrids based on silsesquioxane cyclohexyl trisilanol [STOH; i.e., (c-C_6H_{11})$_7$Si$_7$O$_9$(OH)$_3$] and epoxy resin 4,5-epoxyhexyl-1,2-dimethyl acid diglycidyl ester (TDE-85) were prepared with good compatibility of STOH up to 5 wt % with TDE-85. The blended hybrid resins, with various STOH additions, were cured by 4,4'-diaminodiphenylsulfone, and the curing reactions were investigated with differential scanning calorimetry. The incorporation of STOH increased the curing reaction of TDE-85 for three active hydrogens existing in the STOH molecule. The storage moduli and glass-transition temperatures of the cured hybrid resins were studied with dynamic mechanical analysis. The cured hybrids had higher storage moduli than the pure epoxy resins at lower temperatures and increased slightly even when the temperature was above the glass-transition temperature. Two peaks appearing in tan δ curves indicated the block copolymer structure and two different glass-transition temperatures of the cured hybrid resins. The thermal stability and flame retardancy of the cured hybrid resins were investigated with thermogravimetric analysis and limited oxygen index values, respectively. The results showed that introducing silsesquioxane–OH units into epoxy resins could improve the thermal stability and flame retardancy of the resins. © 2007 Wiley Periodicals, Inc. J Appl Polym Sci 106: 4117–4123, 2007

Key words: blends; flame retardance; resins; thermal properties

INTRODUCTION

Polyhedral oligomeric silsesquioxanes (POSSs) are a class of important inorganic–organic hybrid compounds[1–4] with the general formula [RSiO$_{3/2}$]$_n$.[5–7] POSS monomers possess the structure of cubic–octameric frameworks with eight organic vertex groups, one or more of which are reactive or polymerizable (Fig. 1). The inorganic core gives POSSs high thermal stability, whereas the organic groups are good for improving solubility in common organic solvents or compatibility with an organic matrix.[8] Therefore, POSSs can be dispersed on a molecular level into polymeric systems through blending or polymerization and form nanoreinforced organic–inorganic hybrids.[9–16] Polymers incorporating POSSs are becoming the focus of many studies because of the simplicity of the processing and the excellent comprehensive properties of the hybrid materials.

Epoxy polymers are some of the mostly widely studied engineering thermosets because of their excellent thermal, mechanical, and electrical properties.[17] The incorporation of POSSs with epoxy functionality offers the opportunity to enhance the physical properties for advanced electronic, aerospace, and automotive applications. Many silsequioxane–epoxy composites have been studied.[18–32] Ni et al.[33] prepared organic–inorganic hybrids via the *in situ* polymerization of diglycidyl ether of bisphenol A (DGEBA) and 4,4'-diaminodiphenylmethane in the presence of two structurally similar POSS monomers. The morphologies of the resulting hybrids were dependent on the types of R groups in the POSS monomers. Lee and Lichtenhan[34] reported that the molecular-level reinforcement provided by POSS cages could significantly retard the physical aging process of epoxy resins in the glassy state. Lee and Chen[35] prepared hybrid materials based on octa(2,3-epoxypropyl)silsesquioxane with 4,4'-diaminodiphenylmethane and 5-trifluoromethyl-1,3-phenylenediamine. The results showed that the hybrids had excellent thermal, mechanical, and dielectric characteristics and could be high-performance materials with potential applications in electronic packaging. We prepared a multiepoxy silsesquioxane and formed a highly
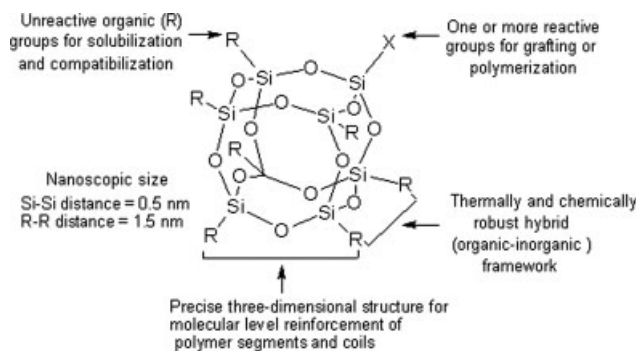
Figure 1 POSS chemical structure.

crosslinked organic–inorganic hybrid silsesquioxane/ bisphenol A dicyanate composite with improved thermal stability and flame retardancy.[36]

POSS silanols possess a hybrid inorganic–organic three-dimensional structure that contains one to four silanol (Si—OH) groups.[37] Fu et al.[38] investigated the influence of phenyl trisilanol polyhedral silsesquioxane (POSS–triol) on the thermomechanical properties and curing of epoxy–amine networks and found that minor amounts of additional POSS–triol resulted in a significant improvement in the glass-transition temperature of epoxy–amine networks. In this study, we prepared a silsesquioxane trilanol with three silanol (Si—OH) groups surrounding the inorganic core, that is, silsesquioxane cyclohexyl trisilanol [STOH; i.e., $(c\text{-}C_6H_{11})_7Si_7O_9(OH)_3$]. STOH was prepared through the incomplete hydrolytic condensation of $CySi(OEt)_3$. The hybrid resins were prepared through the physical blending of STOH with epoxy resin 4,5-epoxyhexyl-1,2-dimethyl acid diglycidyl ester (TDE-85) and cured with 4,4′-diaminodiphenylsulfone (DDS). The performances of the cured hybrid resins, curing reactions, thermal properties, and flammability were examined.

EXPERIMENTAL

Materials

Cyclohexyltriethoxylsilane [$(c\text{-}C_6H_{11})Si(OC_2H_5)_3$], a colorless liquid, was synthesized in our laboratory with a purity of 95%. Concentrated hydrochloric acid was obtained from Xi'an Fine Chemical Plant (Xi'an, China). Anhydrous ethanol was obtained from Tianjin Baishi Chemical Plant (Tianjin, China). Pyridine was obtained from Henan Special Chemical Reagent Plant (Henan, Zhenzhou, China). Ether was obtained from Tianjin FuYu Fine Chemical Corp. (Tianjin, China). DDS was obtained from the Beijing Material Research School (Beijing, China). All these reagents were analytically pure and were used without further treatment. The epoxy resins, DGEBA (epoxy value = 0.52) and TDE-85 (epoxy value = 0.85),

were purchased from Xi'an Resin Plant (Xi'an, China). The chemical structures of the epoxy resins and curing agent are listed in Figure 2.

Analysis methods

IR spectra were acquired on a WQF-310 Fourier transform infrared (FTIR) spectrometer (Beijing Optical Instrument, China). All samples were prepared through the mixing of FTIR-grade KBr with a 1% (w/w) compound and grinding to a fine powder. Spectra were recorded over a 400–4000-cm^{-1} range without baseline corrections. NMR spectra were acquired with an Inova 400 spectrometer at about 20°C. The ^{1}H-NMR spectrum was recorded in a CDCl$_3$ solution at 399.8 MHz. The ^{29}Si-NMR spectrum was recorded in a 1 : 1 (v/v) CDCl$_3$/Et$_3$N mixed solution at 49.7 MHz. Chemical shifts (δ) are reported in parts per million with tetramethylsilane [(Me)$_4$Si] as the standard substance. A mass spectrometry analysis was obtained on a gas chromatography/mass spectrometry apparatus (GC6970-MASS5973) with the electron-impact source method.

Samples for measuring the curing behavior of the hybrids were prepared from a prepreg of silsesquioxane–epoxy/DDS. The prepreg (5–10 mg) was placed in a differential scanning calorimetry (DSC) cell, and the scanning procedures were carried out with a 2910 MDSC V4.4E thermal analyzer coupled to a TA 2000 data analysis system (TA Instruments, Inc., New Castle, DE). The dynamic DSC scanning was carried out up to 350°C at a heating rate of 10°C/min in a nitrogen atmosphere (flow rate = 60 mL/min).
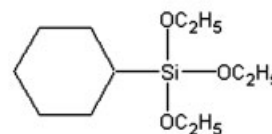
A dynamic mechanical analysis (DMA) of the cured hybrid resin was obtained with a DMA Q800
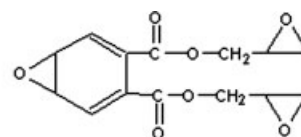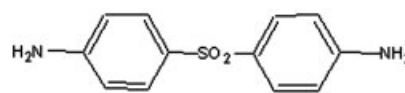
Figure 2 Chemical structures of the main chemical reagents.
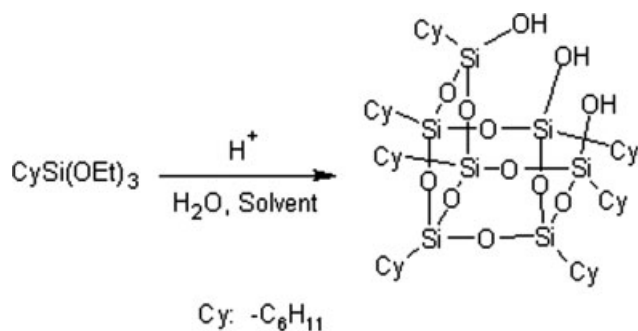
Figure 3 STOH formed from the incomplete hydrolysis condensation of CySi(OEt)$_3$.

system (TA Instruments) operating at 1 Hz at a heating rate of 3°C/min and coupled with the TA 2000 data analysis system. The dimensions of the specimen were $35 \times 10 \times 2$ mm^3.

The thermal stabilities of the cured hybrid resins were tested by thermogravimetric analysis (TGA) with a TGA Q50 Instrument (TA Instruments) under a nitrogen atmosphere. The samples (15–25 mg) were loaded onto platinum pans heated to 600°C (10°C/min/N$_2$). The N$_2$ flow rate was 60 mL/min.

Limited oxygen index (LOI) values were measured on a Stanton Redcraft flame meter (Shenzen, China) according to the standard oxygen index test (ASTM D 2863/77) with sample dimensions of $100 \times 6.5 \times 3$ mm^3. The percentage in the O$_2$–N$_2$ mixture with a flow rate of 16 mL/min that was deemed sufficient to sustain the flame was taken to be the LOI.

Preparation

Preparation and characterization of STOH

Cyclohexyltriethoxylsilane, CySi(OEt)$_3$ (24.6 g, 0.1 mol), and anhydrous ethanol (10 mL) were mixed together to form a solution with a $1M$ concentration. Then, 3 equiv of deionized water (5.4 g, 0.3 mol) was added. Concentrated hydrochloric acid (11 g, 0.3 mol) was used as a catalyst. The reaction solution was stirred at room temperature, and the solution

became turbid. With longer stirring times, the solution turned transparent again; then, heating to 50°C at reflux for 3–5 days led to gelation. A crude product was obtained after the removal of the solvent and washed with ether and pyridine several times; the white, solid silsesquioxane trisilanol was obtained after filtration. The yield of STOH was 2.80 g (20%). The reaction is shown in Figure 3.

Preparation of the blended hybrids

The compositions of the blended hybrids are listed in Table I. The typical processing was as follows. The epoxy resin TDE-85 was preheated to 50°C, and then 0.5–2 wt % STOH was added; the mixture was heated until STOH fully dissolved in the epoxy liquid and formed a transparent solution. The curing agent DDS was also added, and the solution was degassed in a vacuum for 10 min. The aforementioned prepreg was dumped into the mold and cured after the processing, as determined by DSC.

RESULTS AND DISCUSSION

Characteristics of STOH

Figure 4 presents the FTIR spectrum of STOH. The asymmetrical and symmetrical stretching of the methylene groups present as the backbone of the oligomer occurred near 2930 and 2856 cm^{-1}, respectively. The broad band from 3700 to 3100 cm^{-1}, with a maximum at 3400 cm^{-1}, for STOH was primarily ascribed to the stretching of OH of Si—OH groups that were plausibly hydrogen-bonded to other Si—OH groups and water hydrogen-bonded to itself and to the Si—OH groups. The band appearing at 1265 cm^{-1} was due to the overlapping of the asymmetrical bending vibration of the Si—CH$_2$ group; the symmetrical bending vibration appeared at about 760 cm^{-1}. The formation of Si—O—Si bonds in the silsesquioxane was demonstrated by the existence of the Si—O stretching vibration at 1000–1100 cm^{-1}.

TABLE I
Compositions and Properties of Blended Hybrids Based on TDE-85 and STOH

	Hybrid						
	TS0	TS0.5	TS1	TS2	TS3	TS4	TS5
STOH (wt %)	0	0.5	1	2	3	4	5
Solubility of STOH in TDE-85[a]	—	▲	▲	▲	■	■	●
TDE-85 (wt %)	100	99.5	99	98	97	96	95
Curing agent DDS (wt %)	45	45	45	45	45	44	44
5% mass loss temperature (°C)	317	328	330	335	347	357	349
LOI	22.6	23.2	24.8	26.2	28.8	30.9	32.8

The curing conditions were 130°C for 2 h, 180°C for 2 h, 200°C for 2 h, and 220°C for 2 h.
[a] ▲ = soluble at room temperature (a transparent liquid was obtained); ■ = soluble but requiring heating (a transparent liquid was obtained); ● = soluble but requiring continued heating (a translucent liquid was obtained).
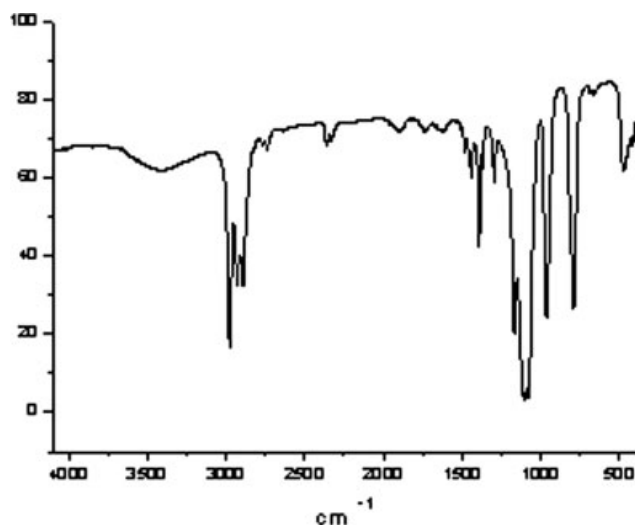
Figure 4 FTIR spectrum of STOH.

Figure 6 Mass spectrum of STOH. [Color figure can be viewed in the online issue, which is available at www. interscience.wiley.com.]

The ^{1}H-NMR spectrum of STOH is shown in Figure 5(a). There was a broad resonance at 6.90 ppm for the three hydrogen-bonded hydroxyl groups of Si—OH. The (c-C_6H_{11})SiOOH proton was at 0.71 ppm. The (c-C_6H_{11})SiO$_{1.5}$ proton was at 1.19 ppm, and the proton of the methylene —CH$_2$— resonances was at 1.73 ppm.

In the ^{29}Si-NMR spectrum of STOH [Fig. 5(b)], two different peaks were found at -60.06 and -69.68 ppm, which were ascribed to the partially condensed —(c-C_6H_{11})SiO(OH) unit and the fully condensed —(c-C_6H_{11})SiO$_{1.5}$ unit, respectively.

The mass spectrum of STOH, covering the molecular ion weight range (m/z) of 600–1000, is shown in Figure 6. The presence of species derived from the loss of one cyclohexyl molecule and one water molecule (871, M^+—C_6H_{11}—H_2O) from STOH and the loss of two cyclohexyl molecules and one water molecule (789, M^+—C_6H_{11}—C_6H_{10}—H_2O) from STOH were confirmed.

Solubility of STOH in TDE-85

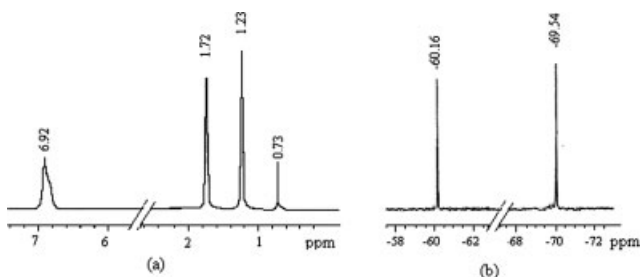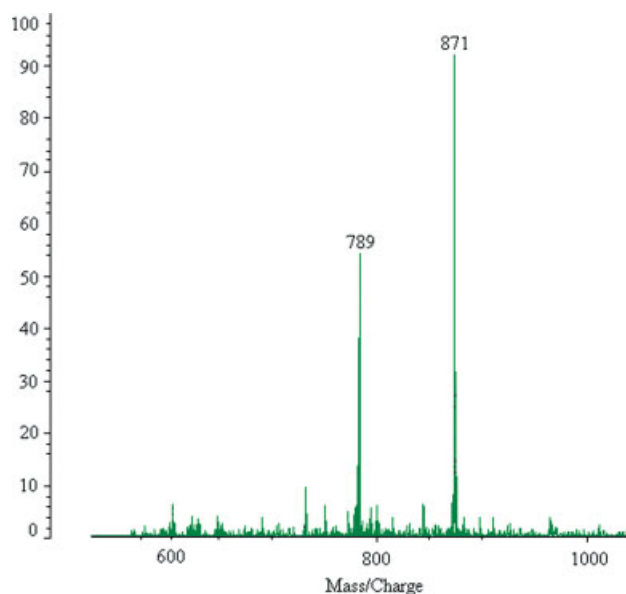STOH was found to have different solubilities in TDE-85 up to 5 wt %, and the details are shown in

Table I. When the STOH content was less than 3 wt %, a transparent liquid was obtained at room temperature. A transparent liquid still could be obtained under heating when the STOH content was 3–4 wt %. However, a translucent liquid was obtained with 5 wt % STOH even when heating was continued. The viscosity of the mixture also increased with increasing STOH content, and the mixture became cloudy when the STOH content was greater than 5 wt %. Although we could increase the amount of STOH dissolved in the epoxy liquids when they were heated, STOH precipitated as the temperature decreased back to room temperature. Therefore, all samples investigated in our study contained less than 5 wt % STOH. In a separate experiment, we found that STOH had less solubility in DGEBA even when heated. We attributed the good solubility of STOH in TDE-85 to the presence of aliphatic groups (cyclohexyl), which resulted in compatibility between STOH and aromatic epoxy TDE-85.

Curing behavior of the blended hybrid resins

Figure 7 presents DSC curves of the blended hybrid resins cured by DDS at a heating rate of 10°C/min. With an increase in the STOH concentration from 0 to 3 wt %, the peak temperature (T_p) decreased from 206 to 193°C. The reduction of T_p indicated that the curing reaction activity of the hybrid resins increased with the addition of STOH. The increase in the curing reactivity was due to the active hydrogens in STOH, which could act as a curing agent for the epoxy resin. Therefore, the hybrid resin had a

**Figure 5** (a) ^{1}H and (b) ^{29}Si-NMR spectra of STOH.
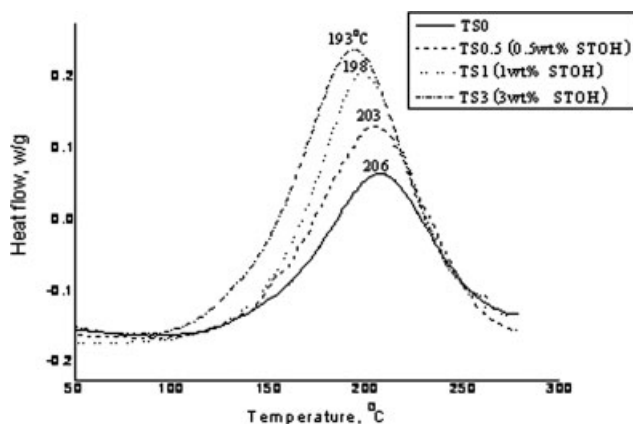
**Figure 7** DSC of the TDE-85–STOH/DDS system at a heating rate of 10°C/min.

higher crosslink density than the pure epoxy resin. To investigate the crosslink densities of the hybrids, FTIR spectra were used to calculate the epoxide conversion, which reflected the crosslink densities of the hybrid resins.

Effect of STOH on the curing process of the blended hybrid resins

Figures 8 and 9 present FTIR spectra of samples TS2/DDS (2 wt % STOH) and TS0/DDS (without STOH) cured at 60°C, respectively. We used the phenyl group stretching peak (1634 cm^{-1}) as the internal standard baseline for the epoxy conversion calculation. The epoxide conversions in the curing process of samples TS2/DDS and TS0/DDS were calculated and are compared in Figure 10. The epoxide conversions were calculated with the area of the epoxide peaks (909 cm^{-1}) at different curing times and normalized with the area of the epoxide peak immediately after mixing. The epoxide conversion of the two samples increased with the curing time increasing. Moreover, the hybrid TS2/DDS (2 wt % STOH)
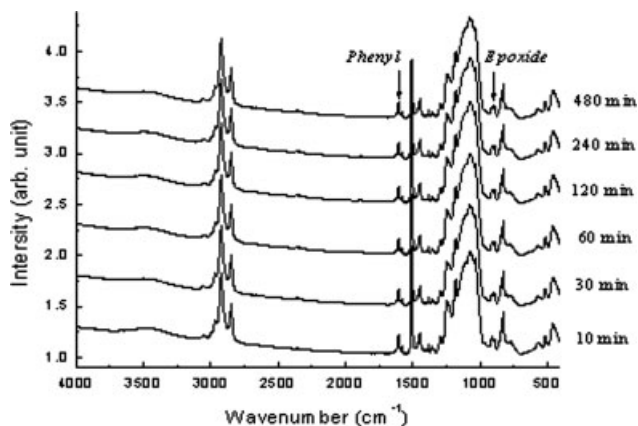
**Figure 8** FTIR spectra of TS2/DDS (2 wt % STOH) cured at 60°C.
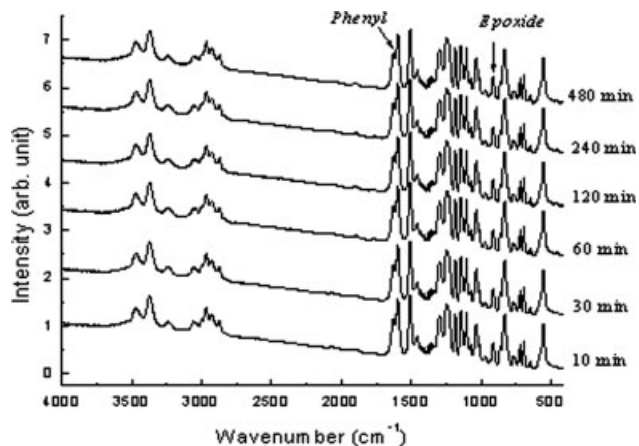
**Figure 9** FTIR spectra of TS0/DDS (without STOH) cured at 60°C.

had a higher epoxide conversion than TS0/DDS (without STOH). After 8 h, the total epoxide conversion was 26.4% in sample TS2/DDS and 24.5% in sample TS0/DDS, as shown in Figure 10. The high epoxide conversion in TS2/DDS indicated that the presence of STOH affected the epoxy–amine reaction and imparted to the hybrids higher epoxy–amine reactivity. The presence of STOH promoted additional crosslinks of the epoxy–amine reaction and resulted in a more highly crosslinked epoxy network with a higher crosslink density. We also show the epoxide conversion of TS3 in Figure 10; the same result was found: a higher epoxide conversion with a higher STOH content. The FTIR results agreed well with our previous results from DSC.

DMA of the blended hybrid resins

Figure 11 presents DMA curves of the blended hybrid resins cured by DDS (storage moduli and tan δ).
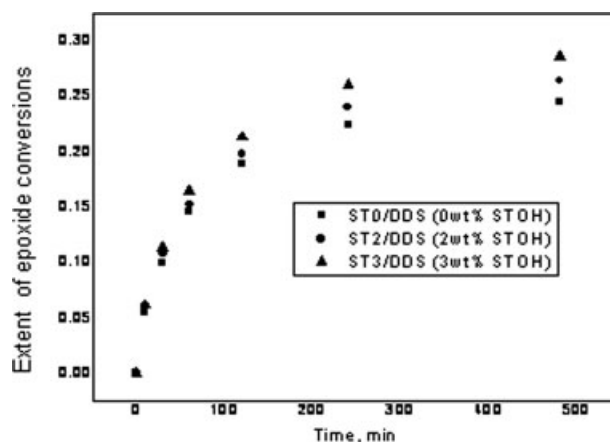
Figure 10 Extent of the epoxide conversion versus time in samples TS2/DDS (2 wt % STOH) and TS0/DDS (without STOH) cured at 60°C.
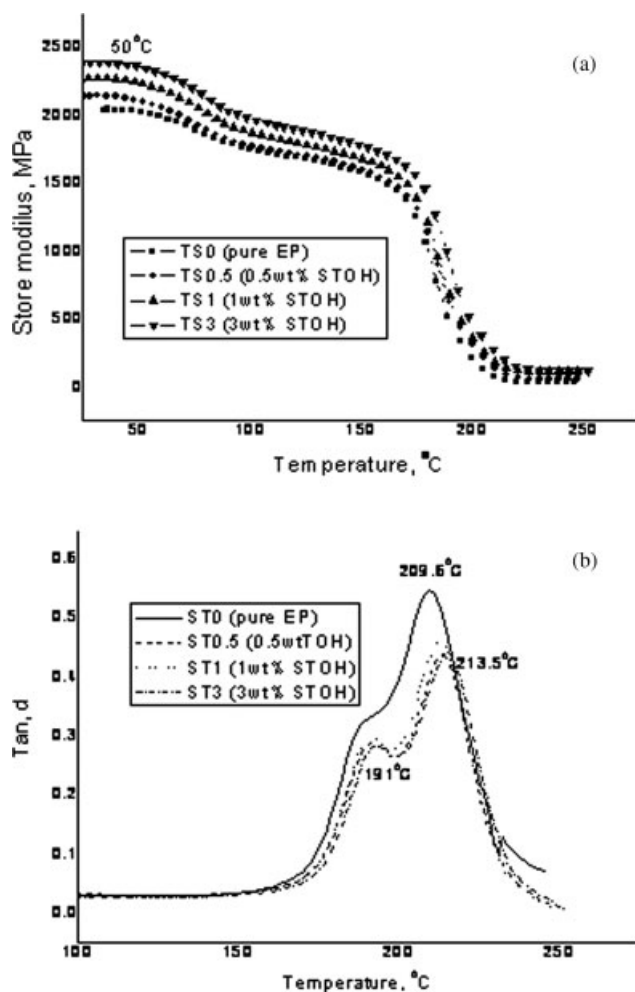
Figure 11 DMA curves of the TDE-85–STOH/DDS system at 3 Hz: (a) storage modulus and (b) tan δ.

Figure 11(a) shows that the hybrids (TS0.5 and TS1) had higher storage moduli than the pure epoxy resin (TS0), especially at a low temperature (<100°C). For example, the storage moduli for TS0.5 and TS1 were 2105 and 2245 MPa at 50°C, respectively, whereas it was 2025 MPa for TS0 at the same temperature. The storage moduli of the hybrids still increased slightly even when the temperature was above the glass-transition temperature. The incorporation of STOH into the epoxy resin made the material stiffer and imparted the ability to resist deformation; as a result, the storage moduli were than higher than that of the pure epoxy resin without STOH.

In Figure 11(b), there are two peaks in the tan δ curves of hybrid resins TS0.5, TS1, and TS3. The temperature in the lower peak was about 191°C, which was lower than the glass-transition temperature of pure epoxy resin TS0 (209.6°C); the temperature in the higher peak was about 213.5°C, which was higher than the glass-transition temperature of TS0. The two glass-transition temperatures of the hybrids indicated the block copolymer structure[39] of

the blended hybrids and the heterogenetic distribution of STOH in the matrix with a low concentration.

Thermal properties of the blended hybrid resin

Figure 12 shows TGA of the cured hybrid resins. The initial decomposition temperature and the char residue obtained from the TGA curves could reflect the thermal stability of the hybrid resins.[40] The initial decomposition temperature was the temperature at which the weight loss was about 5%. The 5% mass loss temperatures of TS0/DDS and TS0.5/DDS were 317 and 328°C, respectively, increasing almost 11°C with only 0.5 wt % STOH. The 5% mass loss temperature increased by 30°C for TS3 with 3 wt % STOH. From Table I, we know that the initial decomposition temperature increased with increasing STOH content in the hybrids and reached the highest value of 357°C for TS4 with 4 wt % STOH; however, the decomposition temperature of the hybrid decreased to 349°C with the higher STOH content of 5 wt %. This might have been caused by the phase separation of the hybrid with a high STOH content. We concluded that the presence of STOH could increase the decomposition temperature and the thermal stability upper limit when the STOH content was 4 wt %. The higher STOH content resulted in a hybrid with a phase-separation matrix and poor properties.

Flame retardancy of the blended hybrid resins

Research has shown that the addition of relatively small amounts of silicon compounds to various polymeric materials can significantly improve their flame retardancy.[41,42] The flame retardancy of the blended resins was investigated through measurements of their LOI values, and the results are shown in Table I. With the STOH contents increasing from 0 to 5 wt %,
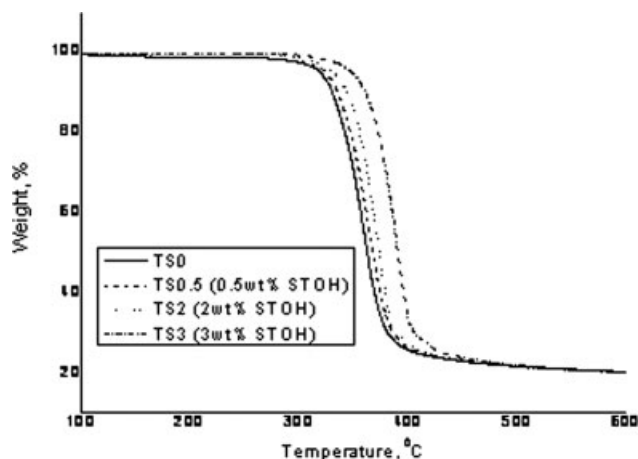
Figure 12 TGA curves of the TDE-85–STOH/DDS system.

the LOI values increased from 22.6 to 32.8; this demonstrated an improvement in the flame retardancy. The incorporation of STOH into the epoxy resins was beneficial for improving the flame retardancy slightly. This performance was based on the concept that the silsesquioxane produced silica (SiO_2) char and interfered with the combustion process during the heating, pyrolysis, ignition, or spread of the flames. Thick char became a better thermal insulating layer, which underwent slow oxidative degradation and prevented heat from reaching the remaining polymer, and eventually led to an improvement in the overall flame retardancy of the hybrid resins.

CONCLUSIONS

An STOH compound was synthesized and successfully introduced into the epoxy resin TDE-85 and formed blended hybrid resins. Hybrid resins cured with DDS were monitored with DSC, and the results showed that the presence of STOH improved the curing reactivity of the epoxy compounds and resulted in a highly crosslinked epoxy network with a high crosslink density. The epoxide conversion was calculated from FTIR spectra, and the results showed that the presence of STOH affected the epoxy–amine reaction and imparted to the hybrids high epoxy–amine reactivity, which resulted in a highly crosslinked epoxy network with a high crosslink density. STOH could act as a cocuring agent for the hybrid curing reaction and formed cured hybrids with a block copolymer structure and two different transition temperatures. The incorporation of STOH gave the epoxy resin good thermal stability, and the thermal stability upper limit for the STOH content was 4 wt %. A higher STOH content resulted in a hybrid with a phase-separation matrix and poor properties. Introducing STOH imparted to the hybrid improved flame-retardant properties.

References

1. Yoshimoto, A.; Takahiro, G. Prog Polym Sci 2004, 29, 149.
2. Kickelbick, G. Prog Polym Sci 2003, 28, 83.
3. Shyue-Tzoo, L.; Stevek, H. J Appl Polym Sci 1996, 62, 1641.
4. Li, G.; Wang, L.; Ni, H.; Pittman, C. U. J Inorg Organomet Polym 2001, 11, 123.
5. Baney, R. H.; Itoh, M.; Sakakibara, A.; Suzuki, T. Chem Rev 1995, 95, 1409.
6. Xu, H.; Xie, P.; Zhang, R. Eur Polym J 2001, 37, 2397.
7. Lu, T. L.; Liang, G. Z.; Kou, K. C. J Mater Sci 2005, 40, 4721.
8. Bharadwaj, R. K.; Berry, R. J.; Farmer, B. L. Polymer 2000, 41, 7209.
9. Bao, Z. N.; Kuck, V.; Rogers, J. A.; Paczkowski, M. A. Adv Funct Mater 2002, 12, 526.
10. Abad, M. J.; Barral, L.; Fasce, D. F.; Williams, R. J. J. Macromolecules 2003, 36, 3128.
11. Lee, A.; Lichtenhan, J. D. J Appl Polym Sci 1999, 73, 1993.
12. Choi, J.; Kim, S. G.; Laine, R. M. Macromolecules 2004, 37, 99.
13. Gilman, J. W.; Schlitzer, D. S.; Lichtenhan, J. D. J Appl Polym Sci 1996, 60, 591.
14. Romo-Uribe, A.; Mather, P. T.; Haddad, T. S.; Lichtenhan, J. D. J Polym Sci Part B: Polym Phys 1998, 36, 1857.
15. Li, G. Z.; Wang, L.; Toghiani, H.; Daulton, T. L.; Koyama, K.; Pittman, C. U., Jr. Macromolecules 2001, 34, 8686.
16. Manna, A. K.; De, P. P.; Tripathy, D. K. J Appl Polym Sci 2002, 84, 2171.
17. Wetzel, B.; Rosso, P.; Haupert, F.; Friedrich, K. Eng Fract Mech 2006, 73, 2375.
18. Xu, H. Y.; Yang, B. H.; Gao, X. Y.; Li, C.; Guang, S. Y. J Appl Polym Sci 2006, 101, 3730.
19. Matejka, L.; Strachota, A.; Plestil, J.; Whelan, P.; Steinhart, M.; Slaof, M. Macromolecules 2004, 37, 9449.
20. Xu, H. Y.; Kuo, S. W.; Huang, C. F.; Chang, F. C. J Appl Polym Sci 2004, 91, 2208.
21. Choi, J.; Yee, A. F.; Laine, R. M. Macromolecules 2004, 37, 3267.
22. Fu, B. X.; Hsiao, B. S.; White, H.; Rafailovich, M.; Mather, P. T.; Jeon, H. G. Polym Int 2000, 49, 437.
23. Wheeler, P. A.; Fu, B. X.; Lichtenhan, J. D.; Weitao, J.; Mathias, L. J. J Appl Polym Sci 2006, 102, 2856.
24. Matějka, L.; Dukh, O.; Kamišová, H.; Hlavatá, D.; Špirková, M.; Brus, J. Polymer 2004, 45, 3267.
25. Lee, Y. J.; Kuo, S. W.; Huang, W. J.; Lee, H. Y.; Chang, F. C. J Polym Sci Part B: Polym Phys 2004, 42, 1127.
26. Liu, H.; Zheng, S.; Nie, K. Macromolecules 2005, 38, 5088.
27. Baldi, F.; Bignotti, F.; Ricco, L.; Monticelli, O.; Riccò, T. J Appl Polym Sci 2006, 100, 3409.
28. Strachota, A.; Kroutilova, I.; Kovarova, J.; Matejka, L. Macromolecules 2004, 37, 9457.
29. Choi, J.; Tamaki, R.; Kim, S. G.; Laine, R. M. Chem Mater 2003, 15, 3365.
30. Choi, J.; Harcup, J.; Yee, A. F.; Zhu, Q.; Laine, R. M. J Am Chem Sci 2001, 123, 11420.
31. Choi, J.; Yee, A. F.; Laine, R. M. Macromolecules 2003, 36, 5666.
32. Laine, R. M.; Choi, J.; Lee, I. Adv Mater 2001, 13, 800.
33. Ni, Y.; Zheng, S.; Nie, K. Polymer 2004, 45, 5557.
34. Lee, A.; Lichtenhan, J. D. Macromolecules 1998, 31, 4970.
35. Lee, L. H.; Chen, W. C. Polymer 2005, 46, 2163.
36. Lu, T. L.; Liang, G. Z.; Guo, Z. A. J Appl Polym Sci 2006, 101, 3652.
37. Xu, H.; Xie, P.; Zhang, R. Eur Polym J 2001, 37, 2397.
38. Fu, B. X.; Namani, M.; Lee, A. Polymer 2003, 44, 7739.
39. Matejka, L.; Dukh, O.; Meissner, B.; Hlavata, D.; Brus, J.; Strachota, A. Macromolecules 2003, 36, 7977.
40. Mantz, R. A.; Jones, P. F.; Chaffee, K. P.; Lichtenhan, J. D.; Gilman, J. W. Chem Mater 1996, 8, 1250.
41. Hsiue, G. H.; Wang, W. J.; Chang, F. C. J Appl Polym Sci 1999, 73, 1231.
42. Liu, Y. L.; Wu, C. S.; Chiu, Y. S.; Ho, W. H. J Polym Sci Part A: Polym Chem 2003, 41, 2354.